

# Fuzzy Cognitive Maps as Naphta Reforming Monitoring Method

R. Larraz and R. Villarroel

University of La Laguna, Chemical Engineering Department, Avda. Francisco Sanchez  
s/n 38200 La Laguna (Spain).E-Mail rlarraz@ull.es

Chrysostomos D Stylios, Ph.D

Lab. for Automation & Robotics. Dep. of Electrical & Computer Engineering  
26500 Rion, Patras, GREECE

**ABSTRACT:** The catalytic reforming of naphta is one of the major refinery processes, designed to increase the octane number of naphta or to produce aromatics. This paper presents a soft computing method for catalytic reforming units performance monitoring. The method is based on Fuzzy Cognitive Maps, which are fuzzy digraph of fuzzy sets, connected by edges. Edge values represent the causal relationship among the concept nodes. As for the problem of how to determine the degree of causal relationship, a differential Hebbian learning developed by improving self-organized learning of neural networks is proposed. A naphta reforming kinetic model is developed for abnormal operation conditions simulation.

**Keywords:** Fuzzy Logic, Catalytic Reforming, Fuzzy Cognitive Maps

## INTRODUCTION

Fuzzy cognitive map (FCM) is an oriented graph showing a causal relationship between different factors, wherein the causal relationship is expressed by either the positive or negative sign for knowledge expressions. FCM expresses the degree of this relationship. Beside a digital version of FCM proposed by Zhang (1988), Taber (1987) et al., proposed a method of inferring the expert weights. Gotoh (1989) used such a method for supporting a plant control system. Pelaez and Bowles (1994) used FCM in Failure Modes Effects Analysis of causes and effects for device failure modes. FCM are employed in QUANTA project to establish an European model of business performance and efectiveness criteria, which complete existing quality models. Perusich and McNeese(1997) used FCM for data abstraction and synthesis in decision making. Kosko and Dickerson (1994) have described undersea virtual world by means of FCM as a dynamical system. This work used FCM as a monitoring tool for a naphta catalytic reforming unit.

## NAPHTA REFORMING

Catalytic reforming converts low-octane virgin and cracked naphtas into high octane gasoline blendstocks. A number of reactions take place during reforming over a dual function catalyst, the predominant reactions are: dehydrogenation of naphtenes into aromatics, cyclization of paraffins, paraffin isomerization and hydrocracking of paraffins. Due to coke deposit the catalyst is regenerated at the end of an operation run. The hydrogen rich gas produced during catalyst reforming is an important byproduct.

The unit consists of three or four adiabatically operated reactors with intermediate heating. After the last bed the reformate is cooled and flashed. The reactors operate at temperatures between 460°C and 540°C, total pressure between 4 and 40 bar and molar H<sub>2</sub> / naphta ratios between 3 and 8. The flash drum operates at 20-40°C.

Catalytic reforming performance is controlled by a wide number of interdependant operating variables (Pistorius, 1985), which makes process modelling a must for proper unit operation and performance monitoring. Process modeling of catalytic reforming can be carried out using correlation models or kinetic models (Turpin, 1992).

Reforming is modelled as regressions of observed data. These equations predict properties useful in the design, operation or evaluation of the unit. The development of correlation models is usually done by individual oil refiners based on their operating experience. Correlations do not give information about the relationship between the operating variables, and, as the catalyst losses activity the coefficient of the equations has to be recalculated. Usually the performance of the unit is evaluated according to a base case.

Kinetic models can easily handle interdependent and forward/reverse reactions, and are excellent tools for predicting individual components yield; they are based on a reaction network, and match the heat and mass balance of the unit integrating the differential kinetic equations of the naphta compounds over the reactors. A proper kinetic model needs

many differential equations and has to group the different hydrocarbon species into lumps for paraffins, naphthenes and aromatics of different carbon number; this fact leads to a complicated mathematical model.

## FUZZY COGNITIVE MAPS IMPLEMENTATION

Fuzzy cognitive maps (FCM) are derived by expanding the cognitive maps proposed by Axelrod (1976). FCM are soft computing tools which combine elements of fuzzy logic and neural networks (Mohr, 1997). As defined by Juliano(1996), an FCM:  $M = (C_M, E_M)$  over the finite universe  $X$  is a fuzzy graph that is a 2-tuple where:

- $C_M \in (0, 1)^X$  is a fuzzy concept space of  $X$ ,
- $E_M$  is a fuzzy multirelation, that is a finite sequence  $(e_1, e_2, \dots, e_M)$  of relations on  $C_M \in (0, 1)^X$ .

Kosko(1986) defines FCM as a dynamical system that relates fuzzy sets and rules. An FCM has the topology of a directed fuzzy graph with cycles or feedback. It is a set of nodes and edges. The concept nodes  $C_i$  are fuzzy sets or even fuzzy systems. The edges  $e_{ij}$  define rules or causal flows  $C_i \Rightarrow C_j$  between the concept nodes. The value of a node reflects the degree to which the concept is active in the system at a particular time. A high numerical value indicates that the concept is strongly present. A negative or zero value - implementations vary - indicates that the concept is not currently active or relevant to the conceptual domain. Two conceptual nodes without a direct link are independent.

A simple FCM showing the relationship among the concepts, Research Octane Number (RON), Reactor Inlet Temperature (RIT) and coke over the catalyst, appears in Figure 1. As the RIT increases the RON increases too, a positive edge among them, but the coke also increases, influencing negatively, and requires higher RIT for the same RON.

Comparing with the tree-structured inference knowledge expression, employed in conventional Expert Systems, FCM are advantageous in respect of higher process rate attainable by its parallel processing capability, easy adaptability to the inference containing feedback, and easy system unification by employing matrix expression(Kahaner, 1990).

FCMs allow users to compare their mental model with the real world, and because of their fuzzy logic elements, extremely forgiving of uncertain information and they are a simple and clear way to represent causal relationships, as process units operators does.

FCM dynamics depends on the dynamics of the concept nodes and causal edges. The edges  $e_{ij}$  are constant weights and the nodes change in time. The state of the map is defined as:

$$C_{t+1} = F(C_t E)$$

where:

$C_t$  is a state vector,  $C = (C_1, C_2, \dots, C_n)$ , with the values of each node of the FCM.

$E$  is the adjacency matrix; an FCM with  $n$  nodes has  $n^2$  edges, which forms a matrix where an entry in the  $(i, j)$  element denotes an edge between nodes,  $i$ , and,  $j$ . If two nodes are independent its edge is zero.

$F$  is the threshold function, we can maintain stability by normalizing the state value. Many threshold functions are available for this normalization; for the purpose of this work, we make the following assumptions:

- Edge values are on the range  $(-1, 1)$ .
- The selected threshold function, the logistic signal function, is a continuous function and provides true fuzzy conceptual node states. the function is:

$$F_i(X_i) = 1 / (1 + e^{-cX_i})$$

where  $X_i = (C_t E)$ .

At large values of the constant,  $c$ , the logistic function approaches discrete threshold functions. We have chosen,  $c = 5$ , as a trade-off which favors the center of the range.

- Input and output values are normalized to a  $(0, 1)$  interval. This is done to avoid threshold function saturation. The transformation is done in two steps; first each data in the data set is recalculated by means of:

$$x' = (x - X) / \sigma$$

where  $X$  is the mean value, and  $\sigma$  is the standard deviation of the data set. Then  $x'$  values are normalized to a  $(0, 1)$  interval due to a linear transformation.

## UNSUPERVISED LEARNING

The similarity of FCMs to neural networks permits unsupervised learning of causal relationships (Kosko, 1997). The differential Hebbian learning law correlates concept changes or velocities. Given a discrete change in a concept value  $\Delta C_i$  at time,  $t$ , and edge strength  $e_{ij}(t)$ , between that conceptual node and the  $j^{\text{th}}$  node in the FCM,

$$\begin{aligned} e_{ij}(t+1) &= e_{ij}(t) + c_t \{ \Delta C_i \Delta C_j - e_{ij}(t) \} & \text{if } \Delta C_i \neq 0 \\ e_{ij}(t+1) &= e_{ij}(t) & \text{if } \Delta C_i = 0 \end{aligned}$$

If the concept values does not change, the edge weight is unchanged. The constant,  $c_t$ , is a learning coefficient which decreases in time, the value of the coefficient is given by

$$c_t(t) = 0.1 \{ 1 - t / 1.1N \}$$

where N is a constant controlling the rate of decrease, we have chosen a value of 5 for this constant. This procedure permits train the FCM with real world data, until the value of the edges adjust the data.

## NAPHTA REFORMING FCM

Given qualitative information about a domain, e.g. operation experience of a particular reforming unit, it is desirable to infer an FCM. The implementation could vary depending on which is the object of the FCM. We have developed a model involving the main reforming operation variables was developed:

- Reactor inlet temperatures; RIT
- Space velocity; LHSV
- H<sub>2</sub>/ naphtha ratio; HHC
- Feed characteristics; naphtha plus twice aromatics, N+2A
- Reactor pressure; P
- Research octane number; RON
- Product ( reformate, gas) yields; C5+, H<sub>2</sub>.

Each of this variables is a node in the FCM, it's value ranges into the operation values and has been normalized in a (0,1) interval; the FCM is shown in Figure 2.

The adjacency matrix E, states the causal relationship into an operation period, each pair (i, j), from the matrix, represents the causal interaction among two variables; as shown in the following table:

*	RIT	LHSV	N+2A	HHC	P	RON	C5+	H <sub>2</sub>
RIT	0	0	0	0	0	+	-	-
LHSV	+	0	0	0	0	-	+	-
N+2A	-	0	0	0	0	+	+	+
HHC	0	0	0	0	0	-	-	-
P	0	0	0	+	0	-	-	-
RON	0	0	0	0	0	0	-	-
C5+	0	0	0	0	0	0	0	+
H <sub>2</sub>	0	0	0	+	0	0	0	0

Model causal relationships may change over time as a result of catalyst deactivation or feed contaminant upset. In this case, it is advisable to periodically infer an FCM and compare the adjacency matrix to detect such changes. The value of the edges can be inferred from the unit operation data by means of unsupervised learning..

## FCM TRAINING

The training procedure for the reforming FCM has been developed in two ways:

- Employing published operation data (Little, 1983).The data covers a naphtha reforming run between regenerations and show the effect of progressive deactivation on unit performance.The run has been divided in several data sets and each set is represented by an adjacency matrix where we can detect causal variations on unit performance.The frequency of FCM training is given by the accuracy of the real data with the calculated ones.The sum square error, R, which represents the error between the predicted and targeted values is employed to evaluate the ability of the network.
- Employing a reforming kinetic model. One of the objects of this work is obtain a method which allows abnormal operation detection in a naphtha reforming unit. This conditions are catalyst deactivation, low or high chloride level over the catalyst, poisoned catalyst, etc....; published operational data of this upsets are difficult to obtain; this has lead us to develop a kinetic model of the naphtha reforming, as a modelling tool for that situations.

## NAPHTA REFORMING KINETIC MODEL

As suggested by Henningsen et al (1970)., a general model of the reforming process is outlined in the following reaction network. The reaction rates are represented by simple first order kinetics in partial pressure of the hydrocarbons, we assume the pressure drop throught the reactors to be unimportant to make our assumption consistent. Naphta components are lumped into the main components: Cracked products, isoparaffins, n-paraffins, 5-ring naphthenes, 6-ring naphthenes and aromaticas. Hydrogen production is calculated stoichiometrically. Gas

composition is calculated from a flash calculation according to Marin et al.(1983),. The proposed reaction model forms a set of differential equations that describes the concentration and temperature profiles in a reforming reactor system:

$$dX/dw = \sum \alpha K_n P_i$$

where X represents a naphta component, w is catalyst weight,  $K_n$  is the kinetic constant for reaction n ,  $\alpha$  is the stoichiometric coefficient for each network reaction and  $P_i$  is the partial pressure of component i.

$$K_n = k \exp(-E/RT)$$

$$k = \pi^x CA AF$$

AF is a catalyst activity factor, CA is the acid level of the catalyst and  $\pi^x$  is a pressure factor. E is the activation energy

$$dT/dw = \sum K_n P_i (-\Delta H_i) / \sum F_i C_{pi}$$

T is the reactor temperature,  $\Delta H_i$  is the heat of reaction,  $C_p$  is the specific heat and  $F_i$  is the molar flow of specie i.

Differential equations system was solved by means of "Gear" method.

The reaction network, the values for the Arrhenius dependency and the heat of reaction are shown in the table. These values has been obtained from Hennigsen et al.(1970), Marin and Froment(1982), Taskar and Riggs (1997), and Kugelman(1976). The type of catalytic active center is also shown. The naphta components are identified by: C, ACP, ACH, NP, IP, AR; corresponding to: cracked products, 5-ring naphthenes, 6-ring naphthenes, n-paraffins, isoparaffins and aromatics.

REACTION	Frequency Factor	Activation Cal/mol	Active Center	Heat of Reaction Cal/mol
NP → C	1.76 E13	55000	Acid	-12000
ACH → NP	3.23 E10	45000	Acid/Metallic	-7300
NP → ACH	1.077 E10	45000	Acid/Metallic	7300
ACP → NP	2.40 E9	45000	Acid/Metallic	-14400
NP → ACPC	1.08 E10	45000	Acid/Metallic	14400
IP → ACH	1.08 E10	45000	Acid/Metallic	9100
ACH → IP	3.23 E11	45000	Acid/Metallic	-9100
IP → NP	3.25 E8	40000	Acid	1900
NP → IP	3.24 E9	40000	Acid	-1900
IP → ACP	1.08 E10	45000	Acid/Metallic	16200
ACP → IP	3.24 E10	45000	Acid/Metallic	-16200
ACH → ACP	1.61 E10	40000	Acid	7100
ACP → ACH	1.61 E9	40000	Acid	-7100
ACH → AR	7.24 E8	30000	Metallic	49900

Inclusion of the AF and AC factors allows the simulation of deactivated catalyst . Catalyst deactivated behaviour is modelled including AF factor into the kinetic equations. AF is a value between (0, 1) that is lower as the catalyst is more deactivated.

As pointed out by Parera et al.(1988), the metallic function suffers a decrease in the beginning of the unit run, during the lineout period, and then is stabilized till the end of the run. Only the acid function could vary due to unit upsets, AC factor variation allows this feature. AC value also varies into (0, 1); where 0 means a 0,6% chloride and 1 is a 1,3 % chloride over the catalyst.

Once we have obtained reforming data from abnormal conditions, the question of how to measure this situation is done. Adjacency matrix are calculated for operational data sets and for deactivated condiction. Edge's values from the data sets and deactivated data are compared and the goodnes of fit among them is measured employing sum square error function. Closer results to deactivated adjacency matrix implies a less active catalyst.

## RESULTS

In Figure 3 some of the operational data are displayed, the data were selected from the middle of the cycle, where deactivation of the catalyst has a low rate. Also naphta components transformation, according the reaction network, into to the reaction system is shown.

Training the proposed FCM with the operational data, and following the outlined procedure, the adjacency matrix is obtained for two data set, the data represents a period of sixty correlative days. The matrixs are shown in Figure 4, correlative matrixs are compared; n°1 and n°2 matrix are similar, a slight increase, 0.36 to 0.42, in the N+2A⇒RON egde could indicate a better quality of the treated charges.

The n°3 matrix shows the deactivation matrix obtained from the kinetic model with a high deactivation coefficient; and the same operational data; changes in the LHSV⇒RON edge, -0.28 to -0.39; also in the RIT⇒RON edge, 0.72 to 0.56;

this changes are a signal of catalyst deactivation, where the influence of RIT increase is lower than before. The  $N+2A \Rightarrow$  RON edge, 0.36 to 0.01, show that quality of the charge has a low influence on the RON. FCM fitting goodness between data set n°1, n°2 and the ideal FCMs for deactivated catalyst is shown. From the results; 0,02 to 0,03; we can conclude that Data Set n°2 matches better deactivated matrix, it represents a more deactivated catalyst performance than Data Set n°1.

A more comprehensive reforming FCM is shown in Figure 5; the model includes a "Cycle Length" node where we can analyze the effect of the operation conditions on the run. Each process unit has its own "bottleneck" points, which influence the global performance; the FCM proposed does not represent any particular unit, and each operator model could vary, including or avoiding the proposed nodes.

## CONCLUSIONS

FCMs are soft computing tools that can be used as cognitive model of decision making process for data synthesis and abstraction. The map is constructed from the cause/effect reasoning of the decision maker about the problem they are addressing. A key advantage of FCMs is that attributes with different metrics can be seamlessly incorporated and compared.

A naphtha reforming monitoring method based on FCM is proposed; the model enables unit troubleshooting and can represent operators thinking in a flexible way. FCM can also be trained using an unsupervised learning algorithm. The comparison among the adjacency matrixes obtained from training show causal changes in the unit performance.

A naphtha kinetic model has been developed for abnormal operation conditions simulation; ideal structures are compared to operational data set by means of a fitting measurement procedure.

## BIBLIOGRAPHY

- Axelrod R.; "Structure of decision, in cognitive maps of political elites"; Princeton Press, 1976  
Gotoh K.; Murakami J.; Yamaguchi T.; Yamanaka T.; SICE Joint Symp. of 15th Syst. Symp. and 10th Knowl. Engn. Symp., pp. 99-104, 1989  
Henningsen J., Bundgaard, Nielson M.; Brit. Chem. Eng., Vol 15, n°11, 1970.  
Juliano B., Bandler W.; "Tracing chains of thought"; Physica Verlag, 1996  
Kahaner D.; "Fuzzy logic and neural networks-Takagi paper" Iizuka'90 report, 1990  
Kosko B.; "Differential hebbian learning"; "Neural networks for computing" American Inst. Phys. Conf. Proc., 1986  
Kosko B.; Fuzzy Engineering, Prentice Hall, Upper Saddle River, N.J., 1997  
Kosko K.; Dickerson J.A.; Presence, Volume 3, N°2, pp. 173-189, 1994  
Kugelman A.M.; Hydrocarbon Proc.; January 1976  
Little D.M.; Catalytic Reforming, PennWell Books, Tulsa, OK, 1983  
Marin G.B.; Froment G.F.; Chem. Eng. Sci., 37(5), 759, 1982  
Marin G.B.; Froment G.F.; Lerou J.J.; De Backer W.; EFCE Publ. Ser. Vol 2; n°27, C117 Paris, 1983  
Mohr S.T.; Master's Project; Rensselaer Polytechnic Institute; Sept. 1997  
Parera J., Querini C., Figoli N.; App. Cat., 44, L1-L8, 1988  
Pelaez C.E.; Bowles J.B.; Third Annual FT&T International Conference, 1994  
Perusich K.; McNeese M.; Internet web page; 1997  
Pistorius J.T.; Oil&Gas Journal, 10 June, 1985  
QUANTA Project 25317, 1998  
Taber W.R.; Siegel M.A.; ICNN'87, Vol. 2, pp. 319-325, 1987  
Taskar U.; Riggs J.B.; AIChE Journal; Vol. 43, n°3, 1997  
Turpin L.E.; Hydrocarbon Processing; June 1992  
Zhang W.; Chen S.; ICNN'88, Vol. 1, pp. 231-238, 1988

Figura 1. RON cause/effect FCM

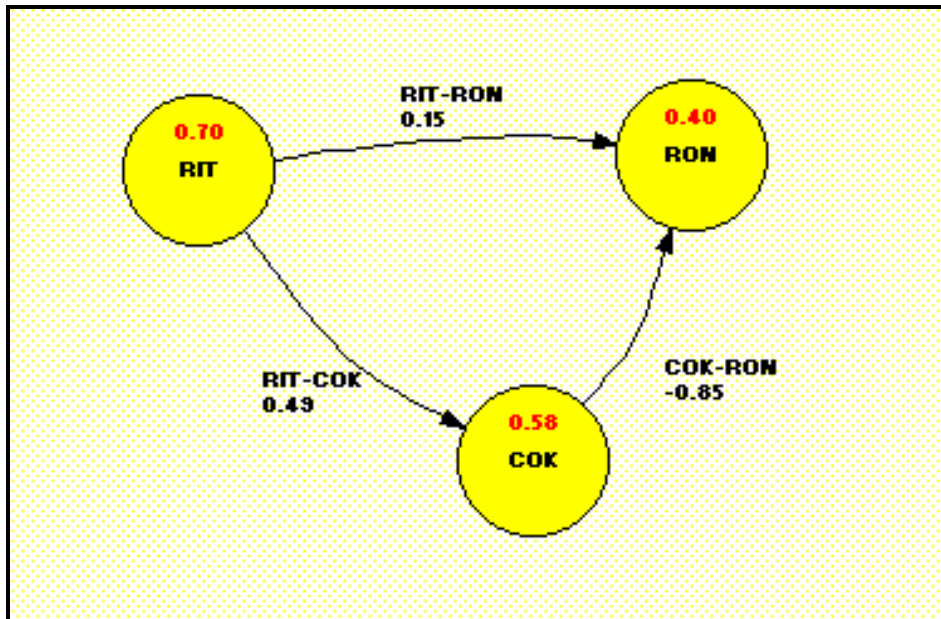


Figure 2. Naphta Reforming FCM

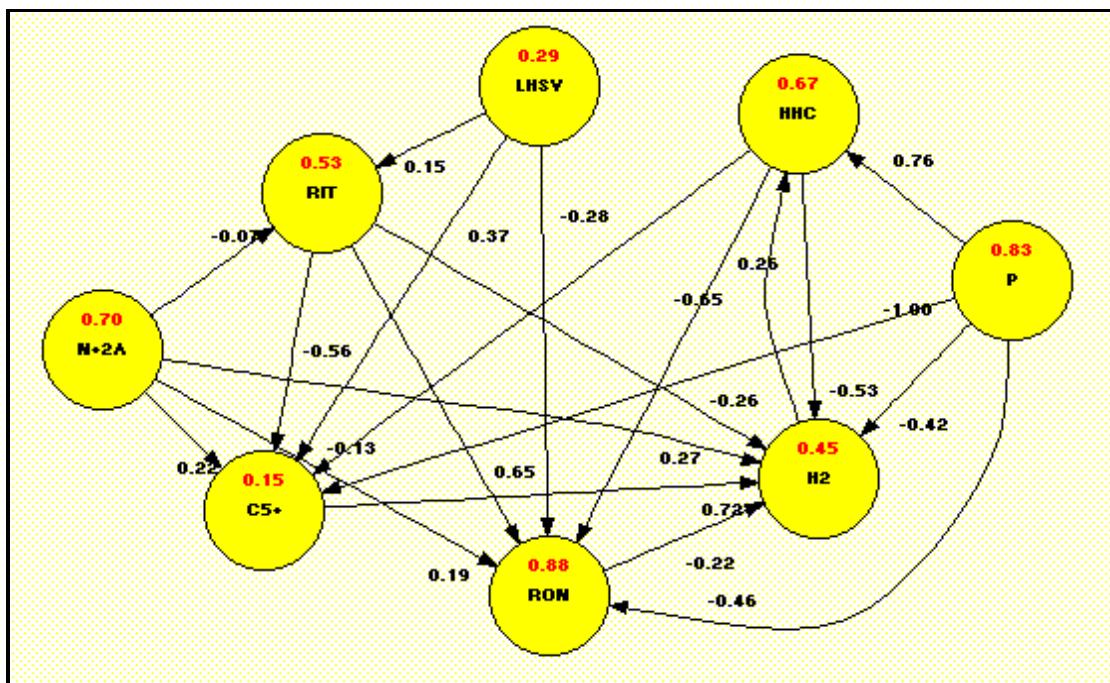


Figure 3

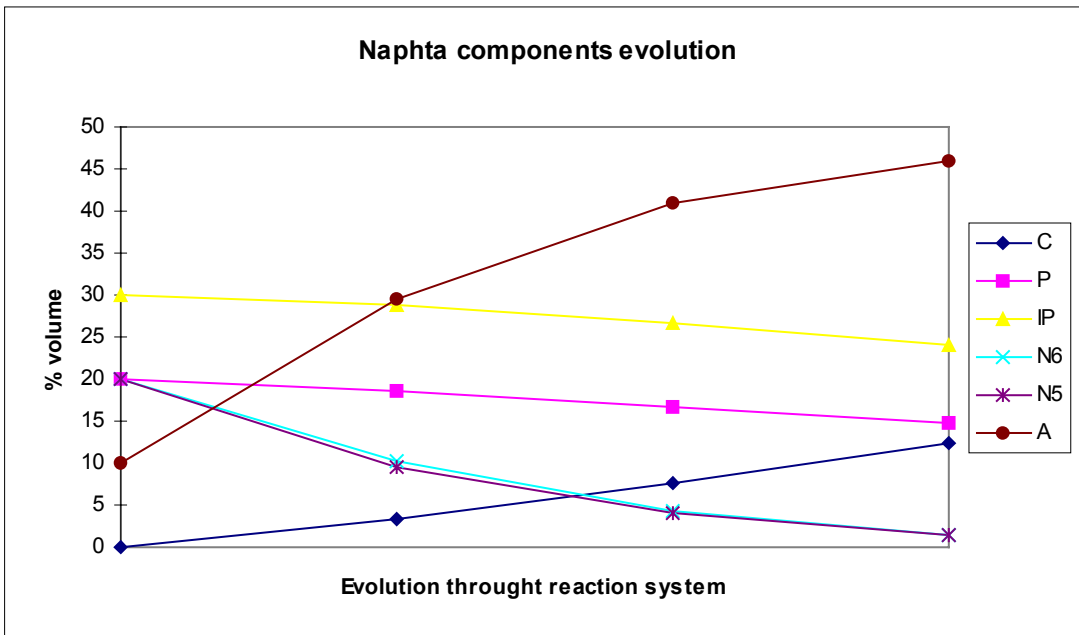
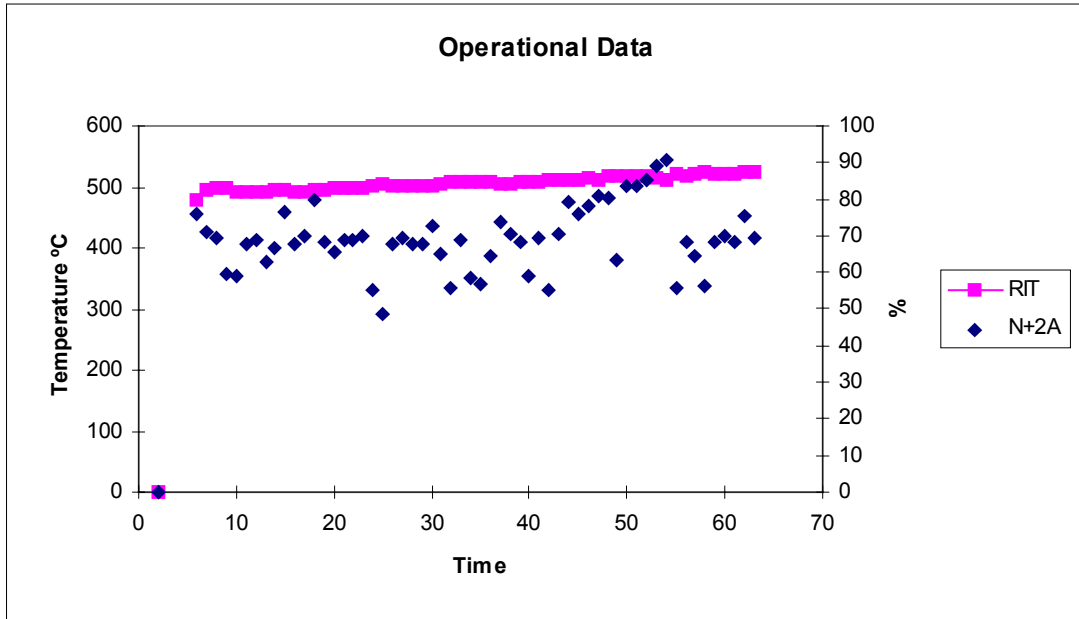


Figure 4 Adjacency Matrix Analysis

**DATA SET n°1**

	<b>LHSV</b>	<b>RIT</b>	<b>N+2A</b>	<b>C5+</b>	<b>RON</b>	<b>H/HC</b>	<b>Pres.</b>	<b>%H<sub>2</sub></b>
<b>LHSV</b>	0	0.12	0	0.37	-0.28	0	0	0
<b>RIT</b>	0	0	0	-0.63	0.72	0	0	-0.26
<b>N+2A</b>	0	-0.09	0	0.22	0.36	0	0	0.27
<b>C5+</b>	0	0	0	0	0	0	0	0.72
<b>RON</b>	0	0	0	0.19	0	0	0	-0.22
<b>H/HC</b>	0	0	0	-0.13	-0.65	0	0	-0.53
<b>Pres.</b>	0	0	0	-1	-0.46	+0.76	0	-0.42
<b>%H<sub>2</sub></b>	0	0	0	0	0	0.26	0	0

**DATA SET n°2**

	<b>LHSV</b>	<b>RIT</b>	<b>N+2A</b>	<b>C5+</b>	<b>RON</b>	<b>H/HC</b>	<b>Pres.</b>	<b>%H<sub>2</sub></b>
<b>LHSV</b>	0	0.12	0	0.36	-0.26	0	0	0
<b>RIT</b>	0	0	0	-0.64	0.74	0	0	-0.27
<b>N+2A</b>	0	-0.09	0	0.19	0.42	0	0	0.28
<b>C5+</b>	0	0	0	0	0	0	0	0.70
<b>RON</b>	0	0	0	0.16	0	0	0	-0.24
<b>H/HC</b>	0	0	0	-0.13	-0.68	0	0	-0.53
<b>Pres.</b>	0	0	0	-1	-0.41	0.67	0	-0.43
<b>%H<sub>2</sub></b>	0	0	0	0	0	0.14	0	0

**DEACTIVATED CATALYST**

	<b>LHSV</b>	<b>RIT</b>	<b>N+2A</b>	<b>C5+</b>	<b>RON</b>	<b>H/HC</b>	<b>Pres.</b>	<b>%H<sub>2</sub></b>
<b>LHSV</b>	0	0.12	0	0.4	-0.39	0	0	0
<b>RIT</b>	0	0	0	-0.60	0.56	0	0	-0.29
<b>N+2A</b>	0	-0.09	0	0.29	0.01	0	0	0.32
<b>C5+</b>	0	0	0	0	0	0	0	0.67
<b>RON</b>	0	0	0	0.29	0	0	0	-0.24
<b>H/HC</b>	0	0	0	-0.19	-0.46	0	0	-0.52
<b>Pres.</b>	0	0	0	-0.91	-0.45	+0.27	0	-0.39
<b>%H<sub>2</sub></b>	0	0	0	0	0	0.09	0	0



### DEACTIVATION MEASUREMENT

Edge	Data Set 1	Data Set 2	Deactivated	$(V_1 - V_d)^2$	$(V_2 - V_d)^2$
	Edges values	Edges values	Edges values		
LHSV-RIT	0.12	0.12	0.12	0.00	0.00
LHSH-C5+	0.37	0.36	0.40	0.00	0.00
LHSV-RON	-0.28	-0.26	-0.39	0.01	0.02
RIT-C5+	-0.63	-0.64	-0.60	0.00	0.00
RIT-RON	0.72	0.74	0.56	0.03	0.03
RIT-H <sub>2</sub>	-0.26	-0.27	-0.29	0.00	0.00
N+2A-RIT	0.09	-0.09	-0.09	0.03	0.00
N+2A-C5+	0.22	0.19	0.29	0.00	0.01
N+2A-RON	0.36	0.42	0.01	0.12	0.17
N+2A-H <sub>2</sub>	0.27	0.28	0.32	0.00	0.00
C5+-H <sub>2</sub>	0.72	0.70	0.67	0.00	0.00
RON-C5+	0.19	0.16	0.29	0.01	0.02
RON-H <sub>2</sub>	-0.22	-0.24	-0.24	0.00	0.00
HHC-C5+	-0.13	-0.13	-0.19	0.00	0.00
HHC-RON	-0.65	-0.68	-0.46	0.04	0.05
HHC-H <sub>2</sub>	-0.53	-0.53	-0.52	0.00	0.00
P-C5+	-1.00	-1.00	-0.91	0.01	0.01
P-RON	-0.46	-0.41	-0.45	0.00	0.00
P-HHC	0.76	0.67	0.27	0.24	0.16
P-H <sub>2</sub>	-0.42	-0.43	-0.39	0.00	0.00
H <sub>2</sub> -HHC	0.26	0.14	0.09	0.03	0.00
<b>Mean Value</b>				0.03	0.02

Figura 5. Complex Naphta Reforming FCM

